

# Triplet state properties of tryptophan residues in complexes of mutated *Escherichia coli* single-stranded DNA binding proteins with single-stranded polynucleotides

Désirée H. H. Tsao,\* Jose R. Casas-Finet,\* August H. Maki,\* and John W. Chase†

\*Department of Chemistry, University of California, Davis, California 95616; and †Department of Molecular Biology, Albert Einstein College of Medicine, Bronx, New York 10461

**ABSTRACT** Complexes of point-mutated *E. coli* single-stranded DNA-binding protein (*Eco* SSB) with homopolynucleotides have been investigated by optical detection of magnetic resonance (ODMR) of the triplet state of tryptophan (Trp) residues. Investigation of the individual sublevel kinetics of the lowest triplet state of Trp residues 40 and 54 in the poly (dT) complex of *Eco* SSB-W88F,W135F (a mutant protein whose Trp residues at positions 88 and 135 have been substituted by Phe) shows that Trp 54 is the most affected residue upon stacking with thymine bases, confirming previous results based on SSB mutants having single Trp → Phe substitutions. (Zang, L. H., A. H. Maki, J. B. Murphy, and J. W. Chase. 1987. *Biophys. J.* 52:867–872). The  $T_x$  sublevel of Trp 54 shows a fourfold increase in the decay rate con-

stant, as well as an increase in its populating rate constant by selective spin-orbit coupling. The two nonradiative sublevels show no change in lifetime, relative to unstacked Trp. For Trp 40, a weaker perturbation of  $T_x$  by thymine results in a sublevel lifetime about one-half that of normal Trp. Trp 54 displays a  $2|E|$  transition of negative polarity in the double mutant SSB complex with Poly (dT), but gives a vanishingly weak  $|D| - |E|$  signal, thus implying that the steady-state sublevel populations of  $T_x$  and  $T_z$  are nearly equal in this residue. Poly (5-BrU) induces the largest red-shift of the *Eco* SSB-W88F,W135F Trp phosphorescence 0,0-band of all polynucleotides investigated. Its phosphorescence decay fits well to two exponential components of 1.02 and 0.12 s, with no contribution from long-lived Trp residues. This

behavior provides convincing evidence that both Trp 40 and 54 are perturbed by stacking with brominated uridine. The observed decrease in the Trp  $|D|$  values further confirms the stacking of the Trp residues with 5-BrU. Wavelength-selected ODMR experiments conducted on the  $|D| + |E|$  transition of *Eco* SSB-W88F,W135F complexed with poly(5-HgU) indicate the presence of multiple heavy atom-perturbed sites. Measurements made on poly (5-HgU) complexes of *Eco* SSB mutants in which each of its 4 Trp residues has been replaced in turn by Phe demonstrate that Trp 40 and 54 are the only Trp residues undergoing stacking with nucleotide bases, as previously proposed (Khamis, M. I., J. R. Casas-Finet, A.H. Maki, J. B. Murphy, and J. W. Chase. 1987. *J. Biol. Chem.* 262:10938–45).

## INTRODUCTION

Optical detection of triplet state magnetic resonance (ODMR) at zero magnetic field has been applied previously to the complexes of *Escherichia coli* single-strand binding protein (*Eco* SSB) with a variety of single-stranded homopolynucleotides (1), providing evidence for the occurrence of stacking interactions between its tryptophan residues and nucleotide bases. These stacking interactions are believed to contribute to the binding and stabilization of the protein-nucleic acid complex. From studies of genetically engineered *Eco* SSB proteins whose tryptophan residues were selectively replaced by phenylalanine, one residue at a time, there is evidence that among its 4 Trp residues at positions 40, 54, 88, and 135, the only stacked Trp residues are Trp 40 and 54 (2). The

identical pattern of stacked Trp residues has been found in an *E. coli* plasmid-encoded SSB protein (3). ODMR studies carried out on wild-type and point-mutated *Eco* SSB proteins bound to poly(deoxythymidylic) acid have shown that there is a unique interaction between Trp 54 and thymine bases in the complex, which produces a reversal in polarity of the Trp 54 ODMR signals and a decrease in the average phosphorescence lifetime (2, 4, 5). Further studies on the triplet state sublevel kinetics of this residue were carried out recently (7), which showed that the decrease in lifetime originates exclusively from the selective enhancement of the  $T_x$  sublevel decay rate.

We have undertaken the preparation by site-directed oligonucleotide mutagenesis (for a review, see reference 8) of a double point-mutation of the *Eco* SSB protein in which Trp residues at positions 88 and 135 have been replaced by phenylalanine. This mutant protein (designated *Eco* SSB-W88F,W135F) contains only the two Trp residues at positions 40 and 54 which we believe function in stacking interactions with single stranded polynucleo-

Dr. Chase's present address is Department of Biochemistry, Case Western Reserve University School of Medicine, Cleveland, OH 44106.

Correspondence should be addressed to August H. Maki.

tides. Here, we report our studies of complexes formed between *Eco* SSB-W88F,W135F and single-stranded polynucleotides.

In the *Eco* SSB-W88F,W135F/poly (dT) complex, studies of the triplet state sublevel kinetics were done monitoring selectively Trp 40 and Trp 54 by choosing appropriate excitation and emission wavelengths. Trp 40 yields ODMR transitions of normal positive polarity, which can be discriminated readily from the negative ODMR signals of Trp 54. From these measurements the triplet state properties of Trp 40 were obtained and compared with those of Trp 54. A reduction of both the  $T_x$  sublevel lifetime and average triplet state lifetime of Trp 40 were observed, although these were of a smaller magnitude than reductions observed recently for Trp 54 (7, 9).

We have extended our studies to the investigation of *Eco* SSB-W88F,W135F protein complexes with brominated and mercurated polynucleotides. The triplet state kinetic properties of the stacked tryptophans in these complexes change dramatically as a result of external heavy-atom perturbations in the binding environment (1, 10, 11). These heavy atom effects occur if there is an overlap of the perturber atom and the perturbed molecule wavefunctions, resulting in an enhancement of spin-orbit coupling. The spin-orbit coupling operator varies as  $r^{-3}$  relative to the perturber atom (12), and thus drops off rapidly with increased distance of the perturbed molecule. Therefore, the heavy atom perturbation is a probe of close range interactions. Because the  $T_y$  and  $T_z$  sublevels of Trp are not normally radiative, the  $|D| + |E|$  ODMR signal is not observed in the absence of a heavy atom perturbation; however, the presence of a heavy atom in the vicinity of the chromophore induces these sublevels to decay radiatively, producing a  $|D| + |E|$  signal at  $\sim 4.4$  GHz.

Wavelength-selected ODMR experiments were performed on the complex of *Eco* SSB-W88F,W135F with poly(5-HgU). The observed discontinuity in the plot of peak frequency of the  $|D| + |E|$  transition versus emission wavelength within the 0,0 band confirms that both Trp 40 and 54 are indeed residues involved in stacking with the nucleic acid bases, as suggested earlier (2).

## MATERIALS AND METHODS

### Sample preparation

*Eco* SSB-W88F,W135F was prepared by site-directed oligonucleotide mutagenesis as described by Mark et al. (13). The mutant gene was subsequently cloned into a vector which allows temperature-dependent expression under regulation of the phage lambda leftward promoter. Purification of the mutant protein was done according to previously published procedures for the preparation of wild type *Eco* SSB (14, 15) with minor variations. The sequence of the mutant protein was confirmed by HPLC tryptic peptide mapping and sequencing of the

altered peptides (data not shown). Specific details of the mutagenesis, purification procedures, and protein chemistry will be published elsewhere.

*Eco* SSB-W88F,W135F protein concentration was determined by amino acid analysis. Protein samples were found essentially free (<2%) of contaminants as judged by sodium dodecyl sulfate/polyacrylamide (15%) gel electrophoresis according to the method of Laemmli (16). Poly(5-HgU) and poly(dT) (P. L. Biochemicals, Milwaukee, WI) were used without further purification. According to the manufacturer, >70% of the uridine bases in the poly(5-HgU) supplied are mercurated covalently at the 5-position. Poly(5-BrU) was prepared by reaction of bromine with poly(U) in a modification of the procedure used to prepare poly(5-BrC) (17) as described previously (11). The concentration of the polynucleotide samples was determined spectrophotometrically using the following extinction coefficients (per mol gr of nucleotide): poly(5-HgU),  $\epsilon_{267} = 1.5 \times 10^4 \text{ M}^{-1} \text{ cm}^{-1}$ ; poly(5-BrU),  $\epsilon_{278} = 6.9 \times 10^3 \text{ M}^{-1} \text{ cm}^{-1}$  (18); poly(dT),  $\epsilon_{264} = 8.52 \times 10^3 \text{ M}^{-1} \text{ cm}^{-1}$  (19). Stock solutions were prepared by dissolving the polynucleotide of interest in water. All chemicals were on the highest available purity.

*Eco* SSB-W88F,W135F/polynucleotide complexes were prepared by mixing appropriate volumes of concentrated stock solutions with a 20 mM sodium cacodylate buffer (pH 7.0) containing 10 mM 2-mercaptoethanol, 1 mM EDTA and 0.3 M NaCl, and were incubated at 37°C for 10 min. The final protein concentration in the complexes was  $\sim 1 \times 10^{-4} \text{ M}$ ; polynucleotides were added to a final 16–20:1 molar ratio. Samples contained 30% (vol:vol) glycerol (spectrophotometric grade, Aldrich Chemical Co., Inc., Milwaukee, WI) as cryosolvent.

## Instrumental

Samples were pipetted into 1-mm inside diameter. Suprasil quartz sample tubes (Heraeus-Amersil, Inc., Sayerville, NJ) and placed within a microwave slow wave copper helix terminating a coaxial transmission line. This was then immersed in liquid nitrogen or liquid helium for spectroscopic measurement. The excitation source was a 100 W high pressure mercury arc lamp and housing (model ALH-215; Photochemical Research Associates, London, Ontario, Canada) after a 12 cm  $\text{NiSO}_4$  (500 g  $\text{L}^{-1}$ ) infrared solution filter and a 10 cm monochromator (model H-10; Instruments SA, Metuchen, NJ) operated at a 16 nm bandwidth. Emission at right angle to the excitation path passed through a high pass WG-345-2 glass filter and was collected by a 1 m monochromator (model 2051, GCA/McPherson Instrument Corp., Acton, MA) equipped with either a 600 or 1,800 groove/mm grating (with slits set for 3.0 or 1.5 nm bandwidth, respectively), and detected by a cooled photomultiplier tube (model 9789 QA; Electron Measurements Inc., Neptune, NJ). Data analysis were performed on a PRO-350 microcomputer (Digital Equipment Corp., Maynard, MA) interfaced to a TN-1550 1024-channel signal averager (Tracor Northern, Inc., Middleton, WI). Microwave frequencies were generated by a HP 8350B or HP 8690B sweep oscillators connected to a HP 8349A microwave amplifier (Hewlett-Packard Co., Palo Alto, CA).

## Methods

At liquid  $N_2$  temperature (77 K) rapid spin-lattice relaxation equalizes the triplet sublevel populations, so that the average phosphorescence lifetime can be obtained from the phosphorescence decay measurement. Decays were deconvoluted by a nonlinear least squares Marquardt algorithm designed to minimize the chi-square of the fitting function and whose goodness of fit was monitored via a residuals plot. Quenching of the spin-lattice relaxation is achieved at 1.2 K by pumping on the liquid He bath in which the sample is immersed. All ODMR and low temperature phosphorescence decay measurements were done under

these conditions. In the slow passage ODMR experiment the phosphorescence intensity was monitored while sweeping the microwaves through a pair of triplet sublevels, inducing magnetic resonance transitions in zero magnetic field. The measurements were performed by adjusting the sweep rate so that passage through a transition was slower than the longer-lived triplet sublevel decay time in the resonance pair. Rapid passage effects on slow passage ODMR signals were compensated by extrapolation of the peak frequency to zero sweep rate.

The fast passage ODMR experiments were performed by sweeping the microwaves through a transition faster than the shorter-lived sublevel decay time of the pair. These transient measurements were collected for the *Eco* SSB-W88F,W135F/poly(dT) complex, in order to determine the lifetime of the radiative  $T_1$  sublevel of Trp 40 and 54.

Microwave-induced delayed phosphorescence (MIDP) measurements (20) were performed in order to obtain the nonradiative decay constants for the  $T_1$  and  $T_2$  sublevels in the SSB-W88F,W135F/poly(dT) complex. In MIDP, optical pumping is carried out until all sublevel populations are at their steady state. Then optical pumping is ceased, the sample luminescence decays and at some time delay  $t$ , a microwave pulse is used to excite a transition between a sublevel pair ( $T_1 - T_2$ ,  $T_2 - T_1$ ). This causes a change in signal intensity due to population transfer between the sublevels. The pulse is applied at different delay times, and a semi-log plot of the relative intensity ( $I/I_0$ ) versus time yields a straight line whose slope equals the rate constant of the nonradiative sublevel.

In wavelength-selected ODMR experiments, it is possible to monitor different chromophore sites, based on the fact that the presence of multiple emitting sites may be revealed as a discontinuity in a plot of zero-field splitting parameters versus emission wavelength, even though their phosphorescence bands are not resolved. Discontinuities, when observed within a composite 0,0-band, are due to distinct chromophore populations that undergo different environmental perturbations. Time-resolved ODMR experiments were performed with the mercury-derivatized polynucleotide complexes, since the resulting short-lived perturbed triplet state is able to respond to rapid sweep rates, while the unperturbed triplet states cannot.

## RESULTS

### i *Eco* SSB-W88F,W135F and its poly(dT) complex

The phosphorescence spectrum of the double point-mutated *Eco* SSB-W88F,W135F exhibits a well-resolved

0,0-band which peaks at 411.2 nm (Table 1). Its phosphorescence decay profile shows a major contribution of a component which exhibits a characteristic Trp lifetime of ~6 s (Table 1). This protein produces ODMR transitions at 1.75 and 2.57 GHz ( $|D| - |E|$  and  $2|E|$ , respectively; see Table 1). The  $|D| + |E|$  signal is not observed. Wavelength-selected ODMR experiments performed on the  $|D| - |E|$  signal identify two distinct Trp sites in the protein, with a discontinuity in the plot of frequency versus wavelength at ~413 nm (Fig. 1 A). No discontinuity is observed when monitoring the  $2|E|$  signal as a function of wavelength, however (Fig. 1 B).

The phosphorescence of the SSB-W88F,W135F/poly(dT) complex shows a red-shift of its 0,0-band maximum to 415.1 nm (Table 1). The phosphorescence decay shows a biexponential profile which was resolved into two components whose values are 5.1 s (63%) and 2.6 s (37%) (Table 1). Comparable lifetime components were obtained upon excitation at 312 nm, where tyrosine residues should not be excited. Therefore, the 2.6 s component cannot be attributed to the contribution of Tyr residues to the protein phosphorescence. On the basis of previous studies of the triplet state of Trp 54 in poly(dT) complexes of a single point-mutated SSB protein, W88F, (7), we assign this component to Trp 54 (see below). The 5.1 s component, which is in the range characteristic of Trp residues, is assigned to Trp 40. Further evidence for these assignments is presented below.

The interaction of Trp 54 with thymine bases gives an unusual set of  $|D| - |E|$  and  $2|E|$  ODMR signals of negative polarity (4), whereas for Trp 40, the signals are of normal positive polarity (Fig. 2 A). This difference in polarity allows for identification of either Trp 54 or 40 in the complex. Choosing appropriate excitation and emission wavelengths enabled us to selectively measure these residues ( $\lambda_{exc} = 295$  nm,  $\lambda_{em} = 410$  nm for Trp 40;  $\lambda_{exc} = 312$  nm,  $\lambda_{em} = 418$  nm for Trp 54). The peak frequencies and the zero field splittings for the  $|D| - |E|$

TABLE 1 Tryptophan phosphorescence lifetimes, zero field ODMR frequencies, and zero field splitting parameters in complexes formed between various single-stranded polynucleotides and point-mutated *Eco* SSB proteins

Sample	$\lambda_{0,0}$	Lifetime components*	D-E	2E	D + E	$ D $	$ E $
	nm				GHz		
<i>Eco</i> SSB-W88F, W135F	411.2	5.6 s (82%), 1.6 s (18%)	1.75	2.57	+ <sup>‡</sup>	3.03	1.28
<i>Eco</i> SSB-W88F, W135F/poly(dT)	415.1	5.1 s (63%), 2.6 s (37%)					
Trp 40			1.74	2.58	- <sup>‡</sup>	3.03	1.29
Trp 54			1.57	2.36	- <sup>‡</sup>	2.75	1.18
<i>Eco</i> SSB-W88F, W135F/poly(5BrU)	416.6	1.0 s (56%) <sup>§</sup> , 0.12 s (44%) <sup>§</sup>	1.69	2.33	4.02	2.86	1.16
<i>Eco</i> SSB-W88F, W135F/poly(5HgU)	414.9	<10 ms (87%), 5.6 s (13%)	1.84	2.56	4.40	3.12	1.28

\*Measured at  $\lambda_{0,0}$ .  $T = 77$  K, unless otherwise indicated.

<sup>‡</sup>Signal is not observed.

<sup>§</sup>Phosphorescence measurements were made at 4.2 K.

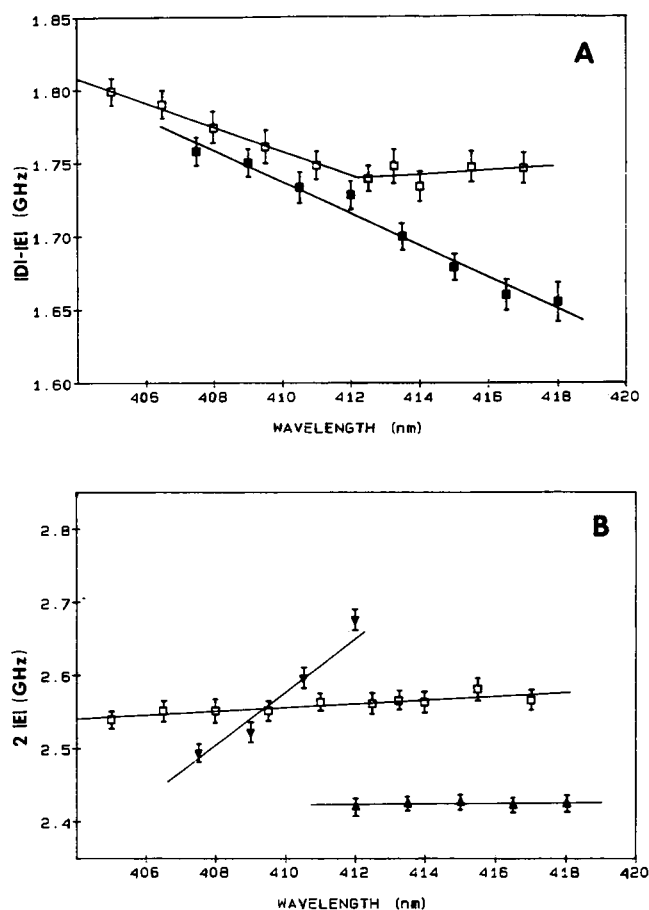


FIGURE 1 (A) Plot of the  $|D| - |E|$  ODMR frequency versus emission wavelength within the 0,0-band in free *Eco* SSB-W88F,W135F ( $1.3 \times 10^{-4}$  M, open squares) and *Eco* SSB-W88F,W135F/poly(dT) ( $1.3 \times 10^{-4}$  M: $2.4 \times 10^{-3}$  M, full squares) (B) Plot of the  $2|E|$  ODMR frequency versus emission wavelength within the 0,0-band in *Eco* SSB-W88F,W135F (open squares) and *Eco* SSB-W88F,W135F/poly(dT) (inverted triangles, positive signals; triangles, negative signals). Excitation was at 295 nm (16 nm bandpass) and emission slits were set at 1.5 nm resolution. Frequencies were corrected for fast passage effects by extrapolation to zero sweep rate. The sample temperature was 1.2 K. Error bars represent  $\pm 5\%$  FWHM (full width at half maximum) of the peak.

and  $2|E|$  transitions of each Trp chromophore in the complex are reported in Table 1. The  $|D| + |E|$  transition was not observed for either of the Trp residues. We did not observe the  $|D| - |E|$  transition for Trp 54 (Fig. 2 A) under steady state conditions. This transition frequency was obtained from a modified nonsteady state slow passage ODMR experiment in which microwaves are swept after cessation of optical pumping and allowing free decay of the sample to occur (data not shown). There is an initial depopulation of the  $T_x$  sublevel before the microwave sweep. The peak frequency is determined after subtraction of a baseline extrapolated from the initial

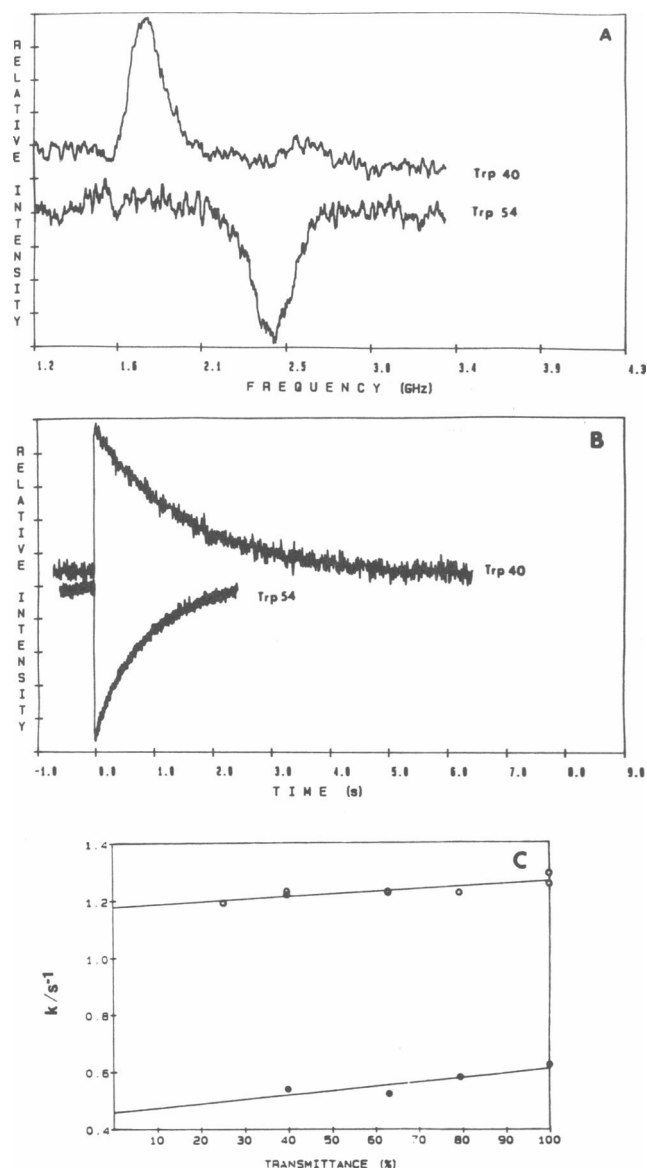


FIGURE 2 (A) Slow passage  $|D| - |E|$  and  $2|E|$  ODMR transitions of Trp 40 and 54 in *Eco* SSB-W88F,W135F complexed with poly(dT). For Trp 40, excitation was at 295 nm, with emission monitored at 410 nm. The sweep rate was  $58 \text{ MHz s}^{-1}$  (10 scans). Trp 54 signals were collected with excitation at 312 nm, with emission monitored at 418 nm. The sweep rate was  $58 \text{ MHz s}^{-1}$  (8 scans). Excitation monochromator slits were set at 16 nm resolution; emission bandpass was 1.5 nm. The sample temperature was 1.2 K. (B) Fast passage ODMR transitions of Trp 40 ( $|D| - |E|$ ) and Trp 54 ( $2|E|$ ). The sweep rate was  $100 \text{ GHz s}^{-1}$  for both Trp 40 (500 scans) and for Trp 54 (1,000 scans). (C) Decay rate constants obtained from fast passage ODMR measurements are extrapolated to zero optical pumping intensity by using a set of neutral density filters. Open circles are data from Trp 54, while closed circles originate from Trp 40.

portion of the phosphorescence decay. When extrapolated to zero sweep rate, the  $|D| - |E|$  transition of Trp 54 was found to be 1.57 GHz (Table 1). This is identical to the value previously reported for the W88F SSB mutant (7).

Fast passage ODMR responses were obtained by sweeping the microwave frequency (sweep rate = 100 GHz s<sup>-1</sup>) through the  $|D| - |E|$  transition of Trp 40 and the 2  $|E|$  transition of Trp 54, during continuous optical pumping. A negative transient response was observed for Trp 54, while for Trp 40 the signal was positive (Fig. 2 B). The fast passage measurements were repeated with a set of neutral density filters in the excitation path, and extrapolated to zero optical pumping (Fig. 2 C) in order to obtain the decay rate constant for the  $T_x$  sublevel of Trp 40 and 54. A single exponential fitting was obtained for both chromophores, because  $T_x$  is the only radiative sublevel (the  $|D| + |E|$  signal is not observed). For Trp 40, we obtained  $k_x = 0.46$  s<sup>-1</sup>, while for Trp 54, it was found that  $k_x = 1.18$  s<sup>-1</sup>.

The nonradiative rate constants for the  $T_y$  and  $T_z$  sublevels of both Trp residues in the Poly (dT) complex were obtained by the MIDP experiment, by pulsing the  $T_y \leftrightarrow T_x$  and  $T_z \leftrightarrow T_x$  transitions, respectively. A typical MIDP response is presented in Fig. 3 A. A plot of the natural logarithm of the ratio of intensities  $I/I_0$  versus the delay time of the microwave pulse is shown in Fig. 3 B, for both Trp residues. The slope of the resulting straight line is equal to the (nonradiative) decay rate constant, assuming that spin-lattice relaxation is negligible. It was found that for Trp 40,  $k_y = 0.076$  s<sup>-1</sup> and  $k_z = 0.041$  s<sup>-1</sup>, while for Trp 54,  $k_y = 0.082$  s<sup>-1</sup> and  $k_z = 0.056$  s<sup>-1</sup>. The kinetic results are summarized in Table 2. The calculated average lifetime ( $\tau_{av}$ ) is  $\tau_{av} = 5.20$  s for Trp 40 and  $\tau_{av} = 2.28$  s for Trp 54. These values are in good agreement with those obtained by analysis of the phosphorescence decay profile at 77 K (Tables 1 and 2).

Pulsed MIDP measurements were performed to obtain the instantaneous relative populating rates,  $p_u$ , of both Trp residues (data not shown). Microwave pulses were applied 30 ms after closing of the excitation shutter, after brief optical pumping (0.2 s). For Trp 54, a microwave-induced decrease of the phosphorescence intensity to half of its initial value (data not shown), indicates that  $p_y$  and  $p_z$ , the populating rates of the  $T_y$  and  $T_z$  sublevels, are negligible compared with  $p_x$ . The same result was obtained previously (7) for Trp 54 in the single point-mutant, *Eco* SSB W88F. For Trp 40, identical experiments show small but detectable  $p_y$ ,  $p_z$  relative to  $p_x$ . These optical responses were difficult to analyze quantitatively, however, since photoselection of Trp 40 is less efficient than that of Trp 54.

Wavelength-selected ODMR experiments performed on the 2  $|E|$  signal of the SSB-W88F,W135F/poly(dT) complex reveal two distinct Trp sites: a wavelength-

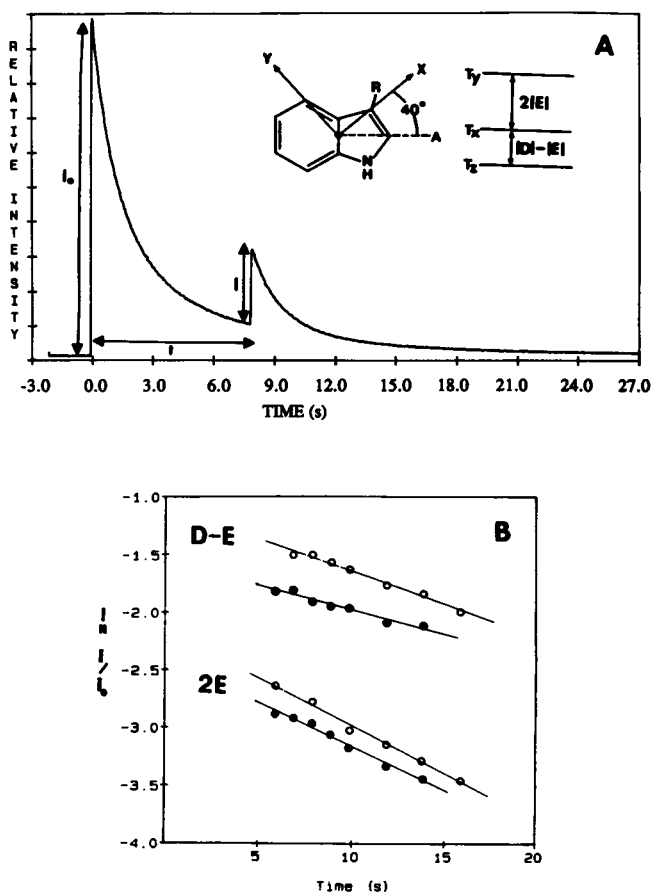


FIGURE 3 (A) MIDP response of Trp 54 in *Eco* SSB-W88F,W135F/poly(dT) complex. The sample was excited at 312 nm with 16 nm bandpass, and monitored at 418 nm with 1.5 nm resolution (signal averaging for 12 scans). (B) Time dependence of the natural logarithm of the MIDP responses for  $|D| - |E|$  and 2  $|E|$  of Trp 40 (filled circles) and 54 (open circles) in the *Eco* SSB-W88F,W135F/poly(dT) complex.

TABLE 2 Comparison of triplet state kinetics of Trp 40 and 54 in *Eco* SSB-W88F, W135/poly (dT) complex with normal tryptophans

Sample	$k_x$	$k_y$	$k_z$	$k_{av}^*$	$\tau_{av}$	Lifetime <sup>†</sup> component
	s <sup>-1</sup>				s	
Trp 40	0.46	0.076	0.041	0.19	5.20	5.1 (63%)
Trp 54	1.18	0.082	0.056	0.44	2.28	2.6 (37%)
RNAse T1 <sup>‡</sup>	0.26	0.076	0.051	0.130	7.69	
Trp <sup>§</sup>	0.24	0.119	0.038	0.134	7.46	

\* $k_{av} = (k_x + k_y + k_z)/3 = 1/\tau_{av}$ .

<sup>‡</sup>Measurement made at 77 K,  $\lambda_{exc} = 295$  nm and  $\lambda_{em} = 415$  nm.

<sup>§</sup>Reference 23.

<sup>†</sup>Reference 24.

independent, low frequency site exhibiting a negative signal which originates from Trp 54, and a strongly wavelength-dependent, high frequency site whose positive signals originate from Trp 40 (Fig. 1 *B*). We were not able to resolve these two sites when monitoring the  $|D| - |E|$  signal (Fig. 1 *A*), since the negative contribution from Trp 54 is buried under the strong Trp 40  $|D| - |E|$  signal of opposite polarity at the excitation wavelength used (295 nm).

## ii SSB-W88F,W135F/poly(5-BrU) complex

The phosphorescence spectrum of the SSB-W88F,W135F/poly(5-BrU) complex shows a red-shift of the 0,0-band maximum to 416.6 nm (at 4.2 K), and is more resolved from the phosphorescence background of 5-BrU bases than it is at 77 K. However, even at 77 K the Trp 0,0-band peaks at  $415 \pm 1$  nm. Therefore, the SSB-W88F,W135F/poly(5-BrU) complex, does not show the pronounced red-shift induced upon cooling the sample from 77 to 4.2 K which has been observed previously for the poly(5-BrU) complexes of wild type and single point mutations of *Eco* SSB protein (1, 2).

The phosphorescence decay profile of the SSB-W88F,W135F/poly(5-BrU) complex (at 4.2 K) was fit to two short components of 1.0 s and 0.12 s (Table 1), indicating the presence of only heavy atom perturbed Trp. Excitation was carried out at 312 nm to avoid the contribution of Tyr residues to the phosphorescence. The proportion of the two decay lifetimes varies across the 0,0-band, being larger for the shorter component at longer wavelengths (Fig. 4). The wavelength-selected phosphorescence half-life plots are identical, however, at 77 K and 4.2 K; the SSB-W88F,W135F/poly(5-BrU) complex lacks the previously observed temperature effect on the decay half-life (2), which was attributed to an energy trapping mechanism.

The SSB-W88F,W135F/poly(5-BrU) complex exhibits the otherwise dark  $|D| + |E|$  slow passage ODMR signal, which must originate from Br-perturbed Trp in the complex (Fig. 5 *A*). A transient response to microwave rapid passage through this signal decays with a lifetime of 0.10 s. Peak frequencies of the ODMR signals and zero field splittings are given in Table 1. It is noteworthy that  $|D|$  and  $|E|$  both decrease with respect to the values in the free protein.

## iii SSB-W88F,W135F/poly(5-HgU) complex

The phosphorescence spectrum of this complex shows a resolved 0,0-band which peaks at 414.9 nm (Table 1). The phosphorescence decay profile exhibits two compo-

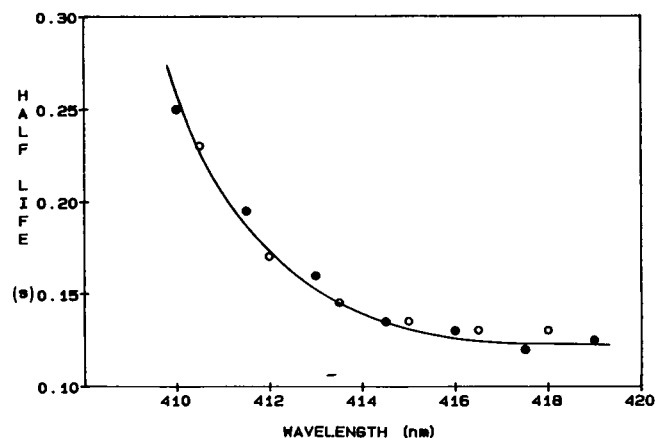


FIGURE 4 Plot of the phosphorescence decay half-life versus wavelength for the complex of poly(5-BrU) ( $2.1 \times 10^{-3}$  M) with *Eco* SSB-W88F,W135F ( $6.9 \times 10^{-5}$  M). Measurements were made at 77 K (open circles) and 4.2 K (filled circles). The sample was excited at 295 nm (16 nm bandpass), and each phosphorescence decay analyzed was the result of 64 accumulations.

nents: one with a lifetime  $< 10$  ms which originates from the Hg-perturbed Trp residues, and another minor component of 5.6 s which originates from Trp residues stacked with nonmercurated bases. Unlike the brominated polyuridylic acid, which is completely derivatized, poly(5-HgU) is only 70% mercurated.

The slow passage ODMR transitions of the SSB-W88F,W135F/poly(5-HgU) complex are shown in Fig. 5 *B*, and the peak frequencies are reported in Table 1. The observed increase in the  $|D|$  value for the Hg-perturbed Trp relative to unstacked Trp is characteristic of perturbation by Hg (21).

The wavelength dependence of the  $|D| + |E|$  transition peak frequency for the *Eco* SSB-W88F,W135F/poly(5-HgU) complex is shown in Fig. 6 *A*. Due to the more symmetric lineshape of the  $|D| + |E|$  signals, all wavelength-selected ODMR plots of poly(5-HgU) complexes presented here have been constructed monitoring this transition. Fig. 6 *A* shows two distinct sites whose transition frequencies are relatively wavelength-independent having a discontinuity at  $\lambda_{em} = 414$  nm. The site which contributes to the blue edge of the 0,0-band is characterized by higher transition frequency (4.37 GHz), while the site which contributes to the red edge displays a lower ODMR transition frequency (4.33 GHz). In order to investigate the individual contributions of Trp 40 and 54 to the wavelength-selected ODMR plot presented in Fig. 6 *A*, singly point-mutated *Eco* SSB proteins were complexed with poly(5-HgU). Because we applied the same rapid sweep rate used for the study of the double point-mutated complex, only the heavy atom-perturbed Trp residue(s) contributed to the signal. In Fig. 6 *B*, plots are

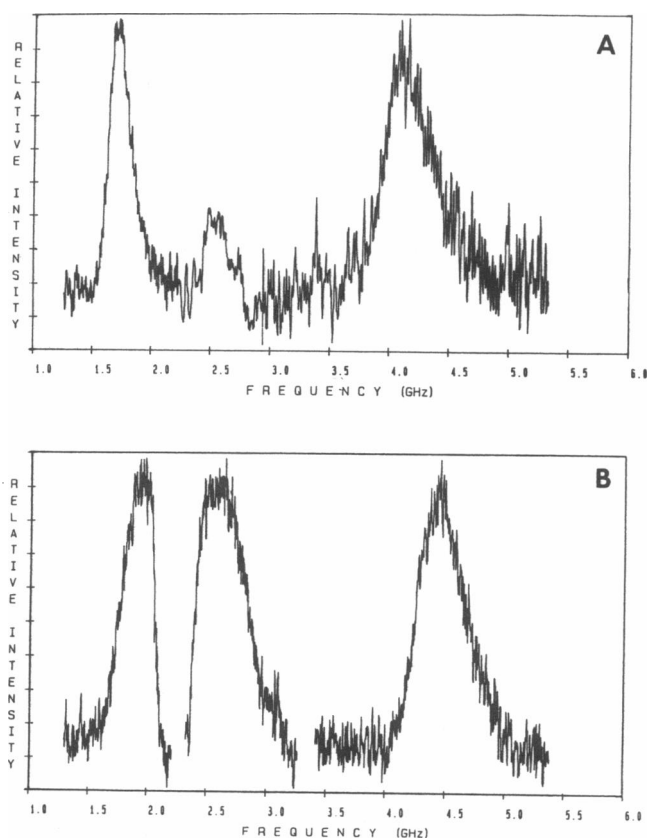


FIGURE 5  $|D| - |E|$ ,  $2|E|$ , and  $|D| + |E|$  ODMR transitions of: (A) *Eco* SSB-W88F,W135F ( $1.4 \times 10^{-4}$  M) complexed with poly(5-BrU) ( $2.3 \times 10^{-3}$  M), and (B) *Eco* SSB-W88F,W135F ( $1.2 \times 10^{-4}$  M) complexed with poly(5-HgU) ( $2.2 \times 10^{-3}$  M). Sample temperature was 1.2 K, and the excitation wavelength was 295 nm (16 nm bandpass). For A the signals were monitored at 417 nm with a sweep rate of  $440 \text{ MHz s}^{-1}$  (800 scans); for B, signals were acquired at 415 nm with a sweep rate of  $20 \text{ GHz s}^{-1}$  (10,000 scans).

presented for the poly(5-HgU) complexes of *Eco* SSB-W54F (squares) and *Eco* SSB-W40F (triangles). Neither one of these systems displays discontinuities in the wavelength-selected ODMR plots, suggesting that in each case only one Trp residue undergoes a heavy atom perturbation, in agreement with previously reported results (2). Moreover, the two perturbed chromophores are characterized by a wavelength-independent transition frequency. Each frequency agrees within experimental error with one of the two sites shown by *Eco* SSB-W88F,W135F/poly(5-HgU). This result demonstrates that the blue-shifted, high-frequency site of the double point-mutated complex originates from Trp 40, while the red-shifted, low-frequency site is due to Trp 54. To provide further evidence for this assignment, *Eco* SSB-W88F was complexed with poly(5-HgU) and studied in a similar way. As shown in Fig. 6 C, the wavelength-

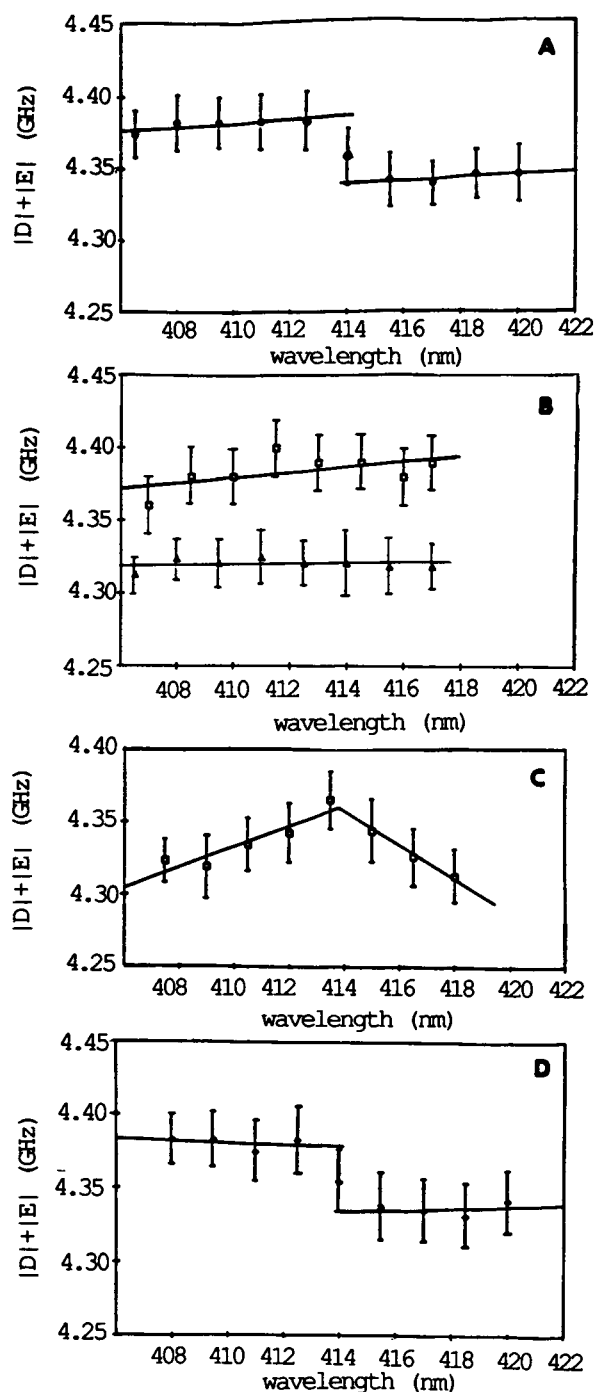


FIGURE 6 Plot of the  $|D| + |E|$  ODMR peak frequency vs. emission wavelength through the heavy atom-perturbed Trp 0,0-band in the complexes of poly(5-HgU) with: (A) *Eco* SSB-W88F, W135F; (B) *Eco* SSB-W54F (squares) and *Eco* SSB-W40F (triangles); (C) *Eco* SSB-W88F; (D) *Eco* SSB-W135F. Microwave sweep rate was  $20 \text{ GHz s}^{-1}$ . Excitation wavelength was 295 nm (16 nm bandpass); emission slits were set at 1 nm resolution. Individual points were acquired after accumulation of 10,000 scans. Error bars are  $\pm 5\%$  FWHM of the peak.

selected ODMR plot of this system exhibits two sites with a discontinuity in slope at 414 nm indicating that Trp 40 and 54 both undergo stacking with 5-HgU bases. In contrast with the double point-mutated protein complex, the two sites now display a wavelength-dependent transition frequency (Fig. 6 C). However, when the poly(5-HgU) complex of *Eco* SSB-W135F is studied, we obtained a plot showing two wavelength-independent sites (Fig. 6 D) that is practically indistinguishable from that of *Eco* SSB-W88F,W135F (Fig. 6 A). Trp 135 is known to be located outside the DNA binding domain (22). Taken together, the wavelength-selected ODMR plots of the poly(5-HgU) complexes of the four singly point mutated Trp  $\rightarrow$  Phe *Eco* SSB proteins and the *Eco* SSB-W88F,W135F mutant show that Trp 40 and 54 are the only Trp residues which undergo heavy atom perturbation in the complexes.

## DISCUSSION

The phosphorescence 0,0-band maximum of the doubly point-mutated *Eco* SSB-W88F,W135F protein is found at  $411.2 \pm 0.2$  nm, while those for wild type *Eco* SSB and *Eco* SSB-W88F are at 412.0 and 411.8 nm, respectively (2). Therefore, though replacement of Trp 88 does not affect the Trp phosphorescence 0,0-band maximum within experimental error, replacement of both Trp 88 and 135 causes a blue shift of 0.8 nm, indicating that the emission of Trp 135 lies to the red of the wild type phosphorescence peak. The observed red-shift of *Eco* SSB-W88F,W135F upon binding to poly(dT) relative to the free protein (3.9 nm) is of the same magnitude as that found for the wild type protein (4.0 nm). The magnitude of this red-shift (2), as well as the appearance of characteristic ODMR signals of negative polarity demonstrate the occurrence of Trp 54 stacking in the poly(dT) complex of the double mutant.

Based on the polarity of the slow passage ODMR signal, it is possible to determine the triplet state kinetic parameters of Trp 40 and 54 upon stacking with thymine bases. The negative steady state ODMR response is indicative of a highly selective intersystem crossing from  $S_1$  to the  $T_x$  sublevel in Trp 54. This sublevel populating pattern has been observed previously (7) and stacking also is known to enhance the radiative character of the  $T_x$  sublevel. In Table 2, we can compare the kinetic properties of Trp 54 and Trp 40 with those of RNase  $T_1$  (a protein which contains a single Trp residue), and free tryptophan. It is evident that Trp 54 is the residue most affected by stacking; the phosphorescence lifetime reduction originates exclusively from the  $T_x$  sublevel, which shows a fourfold reduction of its intrinsic lifetime relative to the  $T_x$  sublevel of normal, unstacked Trp. The other

two nonradiative sublevels of Trp 54 show no significant change in lifetime (Table 2). These values are in very good agreement with previous work, in which the triplet state properties of Trp 54 were determined in a poly(dT) complex of the *Eco* SSB-W88F mutant (7).

Trp 40, on the other hand, shows a smaller perturbation upon complexing with poly(dT). The  $T_x$  sublevel lifetime is reduced likewise from that of normal Trp, while the  $T_y$  and  $T_z$  decay rate constants are unaffected, within experimental error (Table 2). The positive steady state ODMR responses, combined with the individual sublevel decay rate constants suggest that the Trp 40  $S_1 \rightarrow T_1$  intersystem crossing routes do not favor the  $T_x$  sublevel to the same extent that is found for Trp 54.

The calculated average lifetimes of both Trp 40 and 54, presented in Table 2, agree well with the phosphorescence decay components of the *Eco* SSB-W88F,W135F/poly(dT) complex (Table 1), whose decay at 77 K was fitted to a biexponential, giving 5.1 s for Trp 40 and 2.6 s for Trp 54.

The *Eco* SSB-W88F,W135F/poly(dT) complex shows two positive ODMR transitions under conditions which result in photoselection of Trp 40 ( $\lambda_{ex} = 295$  nm,  $\lambda_{em} = 410$  nm). For Trp 54, red-edge excitation with narrow bandpass ( $\lambda_{ex} = 312$  or 318 nm) and monitoring to the red of the phosphorescence 0,0-band maximum yields only a negative signal for the  $2|E|$  transition, while the  $|D| - |E|$  signal is not observed (Fig. 2 A). Negative  $|D| - |E|$  and  $2|E|$  transitions were observed for all the poly(dT) complexes of singly point-mutated *Eco* SSB proteins which contain Trp 54. We can conclude that in the case of *Eco* SSB-W88F,W135F the steady state populations of the  $T_x$  and  $T_z$  sublevels of Trp 54 are not significantly different.

The poly(5-BrU) complex of *Eco* SSB-W88F,W135F shows the largest red shift of the phosphorescence 0,0-band of any SSB mutant so far investigated (2). We believe that the temperature dependence of the phosphorescence lifetime which is observed in poly(5-BrU) complexes of wild type SSB, and in the single Trp  $\rightarrow$  Phe mutants results from a thermal equilibrium distribution of stacked (low energy, short lifetime) sites and unstacked (higher energy, long lifetime) sites (2). Thus, as the temperature is lowered, the lifetime of the phosphorescence which is observed at any wavelength becomes shorter. In order for this phenomenon to occur, two types of Trp residues (stacked and nonstacked) must be present in the complex of the SSB protein with polynucleotides; such is the case for wild-type SSB protein as well as for all the single Trp point-mutations. In the Poly(5-BrU) complex of the double point mutant SSB-W88F,W135F, the phosphorescence lifetime at a given wavelength is the same at 77 K as at 4.2 K (Fig. 4). We believe that this constitutes evidence for the previous interpretation of



thermal equilibration among emitting sites, as well as the stacking (and therefore reduced lifetime) of both Trp 40 and 54. The fact that all the single Trp  $\rightarrow$  Phe mutants show this temperature dependence of the half-life of the Poly (5-BrU) complexes supports the argument that neither Trp 88 or Trp 135 is stacked with 5-BrU.

In the poly(5-HgU) complex of *Eco* SSB the phosphorescence 0,0-band is red-shifted relative to the free protein, while the phosphorescence lifetime is reduced by three orders of magnitude to  $<10$  ms due to a large heavy-atom perturbation. This effect also allows the otherwise dark  $|D| + |E|$  transition to be observed, under rapid sweep conditions. There is an increase in the radiative strength of the triplet sublevels, as a result of spin-orbit coupling. The use of Hg as a perturber causes an increase in the  $|D|$  value of Trp (21) which overwhelms the expected decrease due to stacking.

Wavelength-selected ODMR studies conducted on the poly(5-HgU) complexes of single point-mutated *Eco* SSB proteins (in which each Trp, in turn, has been selectively replaced by Phe) and the double point-mutated *Eco* SSB-W88F,W135F show two Hg-perturbed, wavelength-independent Trp sites which originate from Trp 40 ( $\sim 4.37$  GHz, blue-shifted) and Trp 54 ( $\sim 4.32$  GHz, red-shifted). No other Trp residue is subjected to a heavy atom effect. Although Trp 40 and 54 sites were resolved in previous measurements on *Eco* SSB-W88F (2) by monitoring the  $|D| - |E|$  transition of poly(5-HgU) complexes, Trp 40 was found to emit to the red and Trp 54 to the blue. The opposite is observed by monitoring the  $|D| + |E|$  transition of the *Eco* SSB-W88F,W135F mutant. The reason for this disagreement remains unclear; possibly the absence of Trp 135 in the double mutant affects the stacking behavior of Trp 40 and 54 in this manner. The poly(5-HgU) complex of *Eco* SSB-W88F displays an as yet unexplained wavelength-dependence of the Trp 40 and 54 sites. This behavior is observed only when Trp 135, which is located outside the DNA binding domain of the protein, is simultaneously present in the protein complex.

## CONCLUSION

This study, which is an extension of previous work (7, 9), presents a detailed investigation of the triplet state decay kinetics of Trp residues 40 and 54 in the poly(dT) complex of a double point-mutated *Eco* SSB protein. Optically detected magnetic resonance spectroscopy shows that although both Trp 40 and 54 experience an increase in the average phosphorescence decay constant, the effect is much greater for Trp 54, which exhibits a phosphorescence lifetime of only 2.3 s. This lifetime reduction originates exclusively from a reduction of the decay lifetime of the  $T_x$  sublevel of Trp 54. The molecular

details of the interaction of Trp 54 and 40 with thymine bases are not known, though it seems clear that based on the differences in their decay lifetimes and the opposite polarity of their ODMR signals, they must be significantly different.

The study of a poly(5-BrU) complex of *Eco* SSB-W88F,W135F shows the presence of stacked Trp residues, as evidenced by the short-lived optical transient measured from fast-passage experiments, and the reduction of the  $|D|$  zero field splitting parameter. Comparison of wavelength-selected phosphorescence half-life plots with published work on singly point-mutated *Eco* SSB proteins (2) shows the absence of a previously observed energy trapping mechanism. This, combined with the observation of only short-lived components in the Trp decay profile (of 1.0 and 0.12 s), gives evidence that both Trp 40 and 54 are stacked in the complex.

The involvement of both Trp 40 and 54 in the binding process is confirmed by a wavelength-selected time-resolved ODMR study of *Eco* SSB-W88F,W135F bound to poly(5-HgU). Comparison of this work with that done with 5-HgU complexes of *Eco* SSB mutants in which each of its Trp residues has been replaced in turn by Phe demonstrates that Trp 40 and 54 are indeed the only Trp residues of *Eco* SSB protein undergoing stacking with nucleic acid bases.

The availability of *Eco* SSB mutants affecting every Trp position has allowed us to identify the functional Trp residues, construct a mutant containing only those residues (Trp 40 and 54) involved in stacking, and then to study in detail its interaction with various homopolynucleotides. These types of measurements can be extended to include other aromatic residues that may also be involved in the binding process, as has been previously demonstrated by ODMR studies of the effect of site-directed mutagenesis in the vicinity of Trp 54, leading to the identification of Phe 60 as a functional residue (6).

This work was supported by National Institutes of Health grants ES-02662 to August H. Maki, GM-11301 to John W. Chase, and CA-13330 to John W. Chase.

Received for publication 19 September 1988 and in final form 16 January 1989.

## REFERENCES

1. Khamis, M. I., J. R. Casas-Finet, and A. H. Maki. 1987. Stacking interactions of tryptophan residues and nucleotide bases in complexes formed between *E. coli* single stranded DNA binding protein and heavy atom-modified poly(uridylic) acid. A study by optically detected magnetic resonance spectroscopy. *J. Biol. Chem.* 262:1725-1733.

2. Khamis, M. I., J. R. Casas-Finet, A. H. Maki, J. B. Murphy, and J. W. Chase. 1987. Investigation of the role of individual tryptophan residues in the binding of *E. coli* single-stranded DNA binding protein to single-stranded polynucleotides. A study by optical detection of magnetic resonance and site selected mutagenesis. *J. Biol. Chem.* 262:10938-10945.
3. Casas-Finet, J. R., N.-I. Jhon, M. I. Khamis, A. H. Maki, P. P. Ruvolo, and J. W. Chase. 1988. An *Inc Y* plasmid-encoded single-stranded DNA-binding protein from *Escherichia coli* shows an identical pattern of stacked tryptophan residues as the chromosomal *ssb* gene product. *Eur. J. Biochem.* 178:101-107.
4. Khamis, M. I., J. R. Casas-Finet, A. H. Maki, J. B. Murphy, and J. W. Chase. 1987. Role of tryptophan 54 in the binding of *E. coli* single-stranded DNA-binding protein to single-stranded polynucleotides. *FEBS (Fed. Eur. Biochem. Soc.) Lett.* 211:155-159.
5. Casas-Finet, J. R., M. I. Khamis, A. H. Maki, P. P. Ruvolo, and J. W. Chase. 1987. Optically detected magnetic resonance of tryptophan residues in *Escherichia coli* *ssb* gene product and *E. coli* plasmid-encoded single-stranded DNA-binding proteins and their complexes with poly(deoxythymidylic) acid. *J. Biol. Chem.* 262:8574-8583.
6. Casas-Finet, J. R., M. I. Khamis, A. H. Maki, and J. W. Chase. 1987. Tryptophan 54 and Phenylalanine 60 are involved synergistically in the binding of *E. coli* SSB protein to single stranded polynucleotides. *FEBS (Fed. Eur. Biochem. Soc.) Lett.* 220:347-352.
7. Zang, L.-H., A. H. Maki, J. B. Murphy, and J. W. Chase. 1987. Triplet state sublevel kinetics of tryptophan 54 in the complex of *Escherichia coli* single-stranded DNA-binding protein with single-stranded poly(deoxythymidylic) acid. *Biophys. J.* 52:867-872.
8. Botstein, D., and D. Shortle. 1985. Strategies and applications of in vitro mutagenesis. *Science (Wash. DC)*. 229:1193-1201.
9. Tsao, D., J. R. Casas-Finet, and A. H. Maki. 1988. Effect of stacking interactions with poly(dT) on the triplet state decay kinetics of Trp 40 and 54 of *E. Coli* single-stranded DNA-binding protein. *Biophys. J.* 53:221a. (Abstr.)
10. Cha, T. A., and A. H. Maki. 1982. Influence of the mercury blocking reagent 2-mercaptoethanol on the spectroscopic properties of complexes formed between lysyltryptophyllysine and mercurated poly (uridylic acid). *Biochemistry.* 24:6586-6590.
11. Khamis, M. I., and A. H. Maki. 1986. Investigation of complexes formed between gene 32 protein from bacteriophage T4 and heavy atom-modified single-stranded polynucleotides using optical detection of magnetic resonance. *Biochemistry.* 25:5865-5872.
12. McGlynn, S. P., T. Azumi, M. Kinoshita. 1969. *Molecular Spectroscopy of the Triplet State*. Prentice-Hall, Englewood Cliffs, New Jersey.
13. Mark, D. F., S. D. Lu, A. A. Creasey, R. Yamamoto, and L. S. Lin. 1984. Site-specific mutagenesis of the human fibroblast interferon gene. *Proc. Natl. Acad. Sci. USA.* 81:5662-5666.
14. Chase, J. W., R. F. Whittier, J. Auerbach, A. Sancar, and W. D. Rupp. 1980. Amplification of single-stranded DNA binding protein in *Escherichia coli*. *Nucl. Acids Res.* 8:3215-3327.
15. Chase, J. W., J. J. L'Italien, J. B. Murphy, E. K. Spicer, and K. R. Williams. 1984. Characterization of the *Escherichia coli* SSB-113 mutant single stranded DNA binding protein. *J. Biol. Chem.* 259:805-814.
16. U. K. Laemmli. 1970. Cleavage of structural proteins during the assembly of the head of bacteriophage T4. *Nature (Lond.)*. 227:680-685.
17. Deubel, V., and M. Leng. 1974. Interaction between proflavin and double stranded polynucleotides. *Biochim. Physiol. Pflanz. (BPP)*. 56:641-648.
18. Michelson, A. M., J. Dondon, and M. Grunberg-Manago. 1962. The action of polynucleotide phosphorylase on 5-halogenouridine-5' pyrophosphates. *Biochim. Biophys. Acta.* 55:529-540.
19. Ts'o, P. O. P., S. A. Rapaport, and F. J. Bollum. 1966. A comparative study of polydeoxyribonucleotides and polyribonucleotides by optical rotatory dispersion. *Biochemistry.* 5:4153-4169.
20. Schmidt, J., W. S. Veeman, and J. H. Van der Waals. 1969. Microwave-induced delayed phosphorescence. *Chem. Phys. Lett.* 4:341-346.
21. Cha, T.-A., and A. H. Maki. 1984. Close range interactions between nucleotide bases and tryptophan residues in an *Escherichia coli* single-stranded DNA-binding protein-mercurated poly(uridylic acid) complex. *J. Biol. Chem.* 259:1105-1109.
22. Williams, K. R., E. K. Spicer, M. B. LoPresti, R. A. Guggenheimer, and J. W. Chase. 1983. Limited proteolysis studies of the *Escherichia coli* single-stranded DNA binding protein. *J. Biol. Chem.* 258:3346-3355.
23. Ghosh, S., M. Petrin, and A. H. Maki. 1986. Spin-lattice relaxation in the triplet state of the buried tryptophan residue of ribonuclease T1. *Biophys. J.* 49:753-760.
24. Zuclich, J., J. U. von Schutz, and A. H. Maki. 1974. Direct measurement of spin-lattice relaxation rates between triplet spin sublevels using optical detection of magnetic resonance. *Mol. Physiol.* 28:33-47.